Photoacoustics 3 (2015) 143–150

Contents lists available at ScienceDirect

Photoacoustics

journal homepage: www.elsevier.com/locate/pacs

All-optical photoacoustic microscopy

Sung-Liang Chen [a], L. Jay Guo [b], Xueding Wang [c,*]

[a] University of Michigan-Shanghai Jiao Tong University Joint Institute, Shanghai Jiao Tong University, Shanghai, 200240, China
[b] Department of Electrical Engineering and Computer Science, University of Michigan, Ann Arbor, Michigan, 48109, USA
[c] Department of Radiology, University of Michigan, Ann Arbor, Michigan, 48109, USA

ARTICLE INFO

Article history:
Received 14 July 2015
Received in revised form 6 November 2015
Accepted 13 November 2015

Key words:
Optical ultrasound detection
All-optical detection
Biomedical photoacoustics
Photoacoustic microscopy
Photoacoustic endoscopy

ABSTRACT

Three-dimensional photoacoustic microscopy (PAM) has gained considerable attention within the biomedical imaging community during the past decade. Detecting laser-induced photoacoustic waves by optical sensing techniques facilitates the idea of all-optical PAM (AOPAM), which is of particular interest as it provides unique advantages for achieving high spatial resolution using miniaturized embodiments of the imaging system. The review presents the technology aspects of optical-sensing techniques for ultrasound detection, such as those based on optical resonators, as well as system developments of all-optical photoacoustic systems including PAM, photoacoustic endoscopy, and multi-modality microscopy. The progress of different AOPAM systems and their representative applications are summarized.

Contents

1. Introduction

Photoacoustic imaging has drawn considerable attention recently, and is probably the most rapidly-evolving imaging modality in the last decade [1,2]. By utilizing low ultrasonic scattering, photoacoustic imaging provides a powerful tool for imaging deep tissues at spatial resolutions much higher compared with existing optical imaging technologies. There are two major implementations of photoacoustic imaging based on different image formation methods: reconstruction-based photoacoustic computed tomography (PACT) [3,4], and scanning-based photoacoustic microscopy (PAM) [5,6]. In PACT, an expanded laser beam is used to excite the target object as a whole, and an array of ultrasonic detectors, usually arranged in a circular or a planar geometry, is used to simultaneously capture the emitted ultrasonic waves from different orientations. Reconstruction algorithms [7–9] are then employed to generate the initial pressure distribution which can present the optical absorption contrast in the object. Unlike PACT, PAM generates an image based on point-by-point raster scan along the surface of an object. For each laser pulse, a PAM system usually picks one A-line of time-resolved photoacoustic signal. The photoacoustic signal is emitted either from the acoustic focal zone of a focused ultrasound transducer or the optical focal volume defined by a focused laser beam. Based on which method is used to achieve focusing, PAM is either termed as acoustic-resolution PAM (AR-PAM) or optical-resolution PAM (OR-PAM).

Current PAM systems almost exclusively use piezoelectric transducers, often PZT or PVDF based. Piezoelectric transducers usually operate over a band of frequencies centered at their

* Corresponding author at: Tel.: +1734-647-2728; fax: +1734-764-8541.
E-mail addresses: guo@umich.edu (L.J. Guo), xdwang@umich.edu (X. Wang).

http://dx.doi.org/10.1016/j.pacs.2015.11.001

resonant frequency when the thickness of the piezoelectric material equals to half of the corresponding wavelength. The axial resolution of both OR-PAM and AR-PAM are highly dependent on the maximum bandwidth for photoacoustic signal detection. Therefore, PAM systems equipped with higher frequency transducers usually offer higher axial resolution and hence better capability of "depth sectioning". Higher frequency transducers, however, require thinner and, therefore, more fragile films, which imposes higher requirements in fabrication technologies. Although a maximal bandwidth of ~120% of central frequency has been demonstrated for piezoelectric transducers [10], a nearly full bandwidth stretched from very low (DC) to very high (hundreds of MHz) is still highly restricted.

As an alternative to conventional piezoelectric transducers, optically-acoustic detectors (acoustic detection based on optical methods) hold promise for achieving PAM with higher axial resolution. The principle advantage of optically-acoustic detectors is the intrinsically broad detection bandwidth. Moreover, optically-acoustic detectors facilitate an innovative "all optical" design where both excitation and detection of photoacoustic signals are realized optically, bringing about the idea of all-optical PAM (AOPAM). In previous developments, besides the ultra-broad receiving bandwidth, many other unique advantages of AOPAM over conventional PAM have been demonstrated, such as high sensitivity [11,12], ease of miniaturization [13–15], and possibility for non-contact measurement [16–18].

In this review article, we first describe the mechanisms and characteristics of two major optical interferometers that both have been employed for AOPAM, including microring resonators and Fabry-Perot (FP) etalons. Next, we present the recent advancement in AOPAM. After that, we introduce photoacoustic endoscopy (PAE) based on AOPAM. Then, the current development of multi-modality imaging combined with AOPAM is discussed. At the end, an outlook about AOPAM is described.

2. Optical ultrasound detection

Motivated by the need to observe the ultrasonic field, scientists started to examine the feasibility of optical technology for ultrasound detection starting from the 1960s [19]. Afterwards, the development of optical ultrasound detection has made progress gradually benefited in part from the advances in microfabrication technology and material science. In view of the rapid growth of exploration of biomedical photoacoustic imaging during the past decade, researchers also made attempts to investigate the optical methods for detection of photoacoustic signals. Two representative optical ultrasound detection technologies that have been adapted to photoacoustic imaging are polymer microring resonators and FP etalons.

A polymer microring resonator consists of a ring waveguide closely coupled by a bus waveguide, as shown in Fig. 1a. Light is coupled from the bus waveguide into the ring waveguide. A resonance dip in the transmission spectrum occurs, as shown in Fig. 1b, when the round-trip phase acquired by the guided wave is equal to multiples of 2π. That is,

$$(2\pi n_{eff}/\lambda_c)L = 2\pi m \quad (1)$$

or

$$m\lambda_c = n_{eff}L, \quad (2)$$

where n_{eff} is the effective refractive index of the mode guided inside the ring waveguide, L is the circumference of the ring, and λ_c and m represent the resonant wavelength and resonance order (an integer), respectively. Acoustic waves deform the waveguide shape and change the refractive index of the waveguide, thereby leading to a shift of the resonance dip. By fixing the probing wavelength at a high slope in the transmission spectrum, incident ultrasonic waves are detected by recording the optical output power. A detailed description of ultrasound detection mechanism can be found in [20]. One of the great advantages in ultrasound detection using the polymer microring resonator is low noise-equivalent pressure (NEP) over a broad bandwidth (e.g. 105 Pa over 350 MHz, and 21 Pa over 70 MHz, as reported by the literatures [12] and [11], respectively). Another advantage of this method is the wide angular response which is made possible by the small element size of the microring [11]. Moreover, the receiving sensitivity of the microring is, to a first approximation, independent of its element size. Compared with conventional piezoelectric transducers, the above-mentioned unique features render the microring an excellent detector for particular PAM applications such as PAE imaging of angiogenesis and multi-scale photoacoustic imaging. Functional measurement

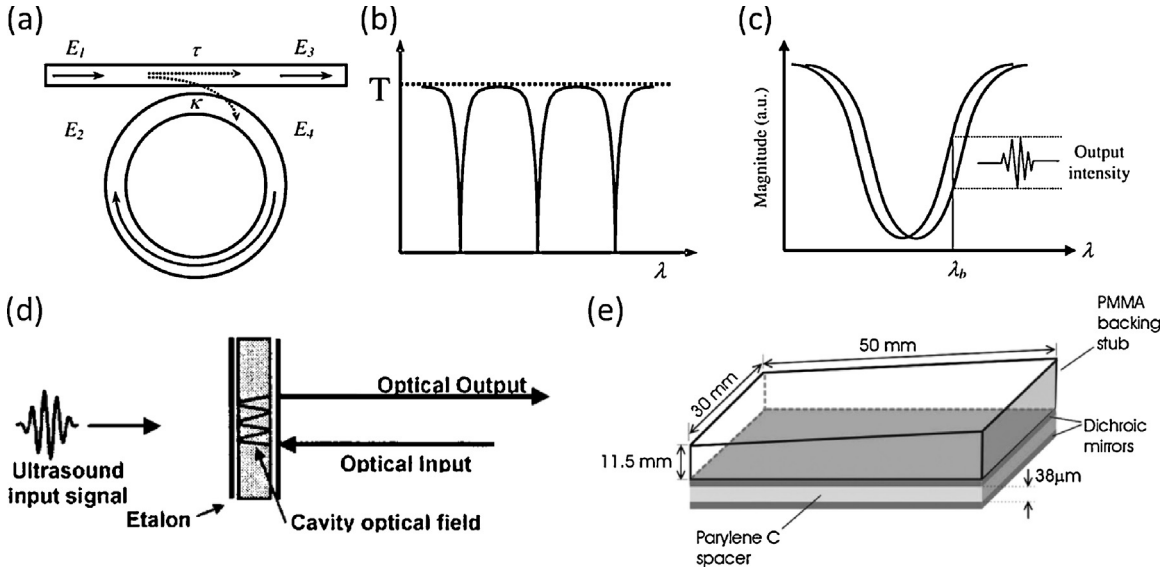

Fig. 1. Examples of optical devices for ultrasound detection. (a) A microring resonator consisting of a ring waveguide and a bus waveguide [20]. (b) Typical transmission spectrum of a microring possesses periodic resonant notches [20]. (c) Ultrasound detection using the optical resonance of a microring sensor [20]. (d) An ultrasound input signal induces thickness modulation of a FP etalon which employs a transparent film sandwiched between a pair of mirrors [24]. (e) A FP sensor head for photoacoustic signal detection [26]. Reprinted with permission from Refs. [20,24,26].

like slow flow speed by microring-based PAM was also demonstrated [21]. In addition, sensitive photoacoustic detection of the microring was utilized to realize efficient real-time detection of pulsed terahertz electromagnetic waves [22].

A FP etalon, an alternative approach for optical resonant ultrasound detection, has also been explored for its application in AOPAM. The FP etalon employs an optical interferometer formed by a transparent film sandwiched between a pair of mirrors [23–27], as shown in Fig. 1d. Acoustically induced changes in the film thickness of the FP etalon modulate the reflected power of an incident laser beam. The FP etalon shares some merits as the microring, such as broadband response from DC to tens of MHz and size-independent detection sensitivity. A detailed description of ultrasound detection mechanism can be found in [23]. One unique feature of the FP etalon which is different from the microring is that the ultrasound detection of the FP etalon is achieved through a free-space interrogation laser beam, leading to exclusive advantages in AOPAM. For example, through raster scan of an interrogation laser beam, photoacoustic signals can be received from a two-dimensional (2D) planar surface [26], as shown in Fig. 1e.

The microring resonator and the FP etalon have been investigated to achieve optimal acoustic detection in PAM. The bandwidth is determined by the film thickness of optical waveguides for the microring resonator and by the transparent film thickness between a pair of mirrors for the FP etalon. The film thickness of the microring resonator can be made very thin through micro- or nano-fabrication technologies [12] and is independent of sensitivity; while the optimal thickness for the FP etalon is really a trade-off between bandwidth and sensitivity [28]. Thus, the microring resonator has the advantage of ultrabroad bandwidth with high sensitivity over the FP etalon. As a comparison, an NEP of 105 Pa has been achieved by the microring resonator over a 350 MHz bandwidth [12], while a similar NEP of 100 Pa has been achieved by the FP etalon with a relatively narrower bandwidth of 20 MHz [29]. However, the detection element size of the FP etalon, defined by the focal spot of a probe laser beam, can be very small, enabling wider ultrasound receiving angles over the microring resonator [29]. The size reduction of the microring resonator is highly restricted by the incurred bending loss, which notably reduces the sensitivity [30].

3. Photoacoustic microscopy

Depending on its lateral resolution decided by optical focusing or acoustic focusing, PAM can be classified as either OR-PAM or AR-PAM. In OR-PAM, the lateral resolution is limited by optical diffraction and can be as fine as submicrometers before the focused beam is distorted by optical scattering. The imaging depth of OR-PAM is usually within 1 mm in optically scattering biological tissues. Its high lateral resolution enables label-free imaging at cellular or sub-cellular level, such as biconcave structure of red blood cells [31,32], mitochondria in fibroblasts and melanosomes in melanoma cells [33]. Axial resolution of OR-PAM is usually limited by detector bandwidth. The microring ultrasound detector with a high quality factor on the order of 10^5 was developed by imprinting technique [11,12,20,34], as shown in Fig. 2a, which facilitates a NEP of 105 Pa over an ultrabroad bandwidth of 350 MHz, as demonstrated in Fig. 2b. The sub-3 μm axial

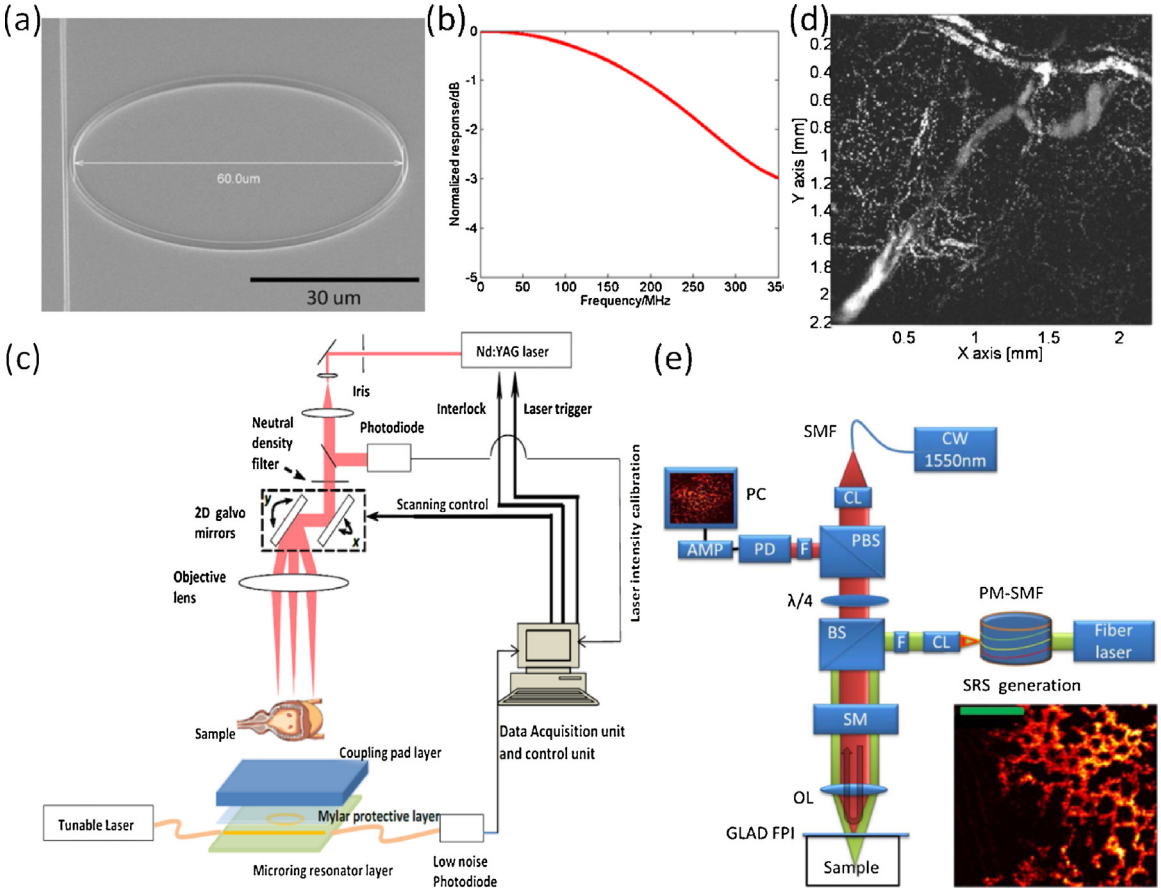

Fig. 2. OR-PAM relying on optical ultrasound detection. (a) An angle view scanning electron microscope image of a microring with a diameter of 60 μm [12]. (b) The frequency response of the microring detector [12]. (c) Schematic of an AOPAM system based on the microring detector [35]. (d) *Ex vivo* images (maximum amplitude projection) of the vasculature in a mouse bladder wall acquired with the AOPAM in (c) [35]. (e) Experimental setup of a GLAD AOPAM system. The inset: an *in vivo* image of the capillary bed in the CAM membrane of 5-day chicken embryo model (Scale bar: 100 μm) [42]. Reprinted with permission from Refs. [12,35,42].

resolution has been demonstrated in photoacoustic imaging using the microring detector [12], which is more than a 2-fold improvement with respect to the reported record based on piezoelectric transducers [37]. The schematic of an AOPAM system based on a microring detector is shown in Fig. 2c [35]. In this system, the laser beam from a Nd:YAG laser (SPOT-10-200-532, Elforlight) was raster scanned over the tissue by 2D galvanometers. Working in a transmission mode, the microring resonator was covered by a Mylar protective layer to avoid potential damage on the microring device due to the focused laser beam. Images of a mouse ear *in vivo* and mouse bladder *ex vivo* (Fig. 2d) were acquired using the system. In Fig. 2d, slight nonuniformity is due to the field of view in the laser-scanning OR-PAM system [36]. Since Fig. 2d was acquired *ex vivo*, red blood cells were not flowing, producing discontinuous pattern in capillaries. A transparent broadband microring resonator was also investigated to facilitate AOPAM performed in a reflection mode [13,38]. Moreover, a systematic study of the distance dependent detection characteristics of the microring-based AOPAM was also conducted [39].

Qualitatively, small detector element size enables wide ultrasound receiving angles, which produces a large field of view. Axial resolution is determined by the bandwidth of the ultrasound pulse, and is degraded with increasing depth due to the acoustic attenuation in water, especially for the high-frequency ultrasonic wave [40]. A quantitative analysis about field of view has been done in [39]. For the microring with a diameter of 60 μm, the field of view in AOPAM is ~20 μm and ~200 μm for the near-field region (distance = 45 μm) and the far-field region (distance = 450 μm), respectively, considering steady-state response to the continuous ultrasonic wave at the frequency of 100 MHz. Besides, the detected bandwidth of photoacoustic signals is ~205 MHz and ~160 MHz for the near-field case (distance = 45 μm) and the far-field case (distance = 450 μm), respectively, which was obtained by experiments [39].

Using FP etalons for optical ultrasound detection, a high-resolution reflection-mode AOPAM system has been developed [41,42]. The FP etalon was fabricated using low-acoustic impedance glancing angle deposited (GLAD) films on either side of a Paralene C layer. The GLAD method allows low acoustic impedance FP devices for highly sensitive ultrasound detection, leading to a NEP of 80 Pa and bandwidth of 18 MHz. The performance of the AOPAM system shown in Fig. 2e was demonstrated by *in vivo* imaging of the capillary bed in chorioallantoic membrane (CAM) of 5-day chicken embryo (Fig. 2e inset). In another study, a fiber optic FP ultrasound sensor was employed in a laser-scanning OR-PAM system with a large field of view (11 mm in diameter) [29]. The sensor does not suffer from the limitation of size-dependent sensitivity and thus can provide high detection sensitivity (NEP < 100 Pa over a 20 MHz bandwidth) with a large angular detection aperture owing to its small active element size (~10 μm).

Besides the microring resonator and the FP etalon, optical ultrasound detection has also been achieved using a noncontact method [43]. Noncontact PAM has many advantages by eliminating the need of acoustic coupling, and is attractive for many applications such as disease diagnosis in ophthalmology and imaging of affected area in surgical operation. Noncontact PAM based on laser interferometers measures the small displacement on the sample surface induced by photoacoustic waves. A noncontact AOPAM using a low-coherence interferometer for acoustic detection has been developed. Its performance was demonstrated through *in vivo* imaging of blood vessels of a mouse ear [16,44]. Lateral resolution of 11 μm and axial resolution of 20 μm was achieved. Another noncontact AOPAM system with a GHz bandwidth and a fine lateral resolution of ~0.48 μm were achieved using a Michelson interferometer [45]. A comparison of ultrasound detection technologies in PAM, including optical ultrasound detectors and piezoelectric detectors, is provided in Table 1.

AR-PAM, by taking advantage of weaker acoustic scattering, provides good image quality at depth beyond the optical diffusion limit up to several centimeters. AR-PAM can also be realized through the optical ultrasound detection and image reconstruction. AR-PAM using a reconstruction algorithm is also called PACT. For example, a microring-based AOPAM system used a synthetic-aperture focusing technique to realize acoustic focusing for AR-PAM [47]. Similarly, digitally-acoustic focusing was also implemented using a photoacoustic scanner based on a planar FP polymer film ultrasound sensor [26,48], as shown in Fig. 3a. The reconstruction algorithm was used in this imaging system (i.e., PACT). *In vivo* high-resolution three-dimensional imaging of the microvasculature was also demonstrated (Fig. 3b and 3c) using this system. Another work used a low-coherence interferometer to realize a noncontact imaging system [49]. The small element size of the optical ultrasound detectors facilitates a wide receiving angle of photoacoustic signal. In combination with the detectors' high sensitivity and broad bandwidth, optical ultrasound detection greatly benefits AR-PAM in improved image quality.

The advantage of AR-PAM with detector arrays is the potential to image in real time with high frame rates. As a feasibility study, a one-dimensional array consisting of four microrings was demonstrated using wavelength-division multiplexing for addressing each element [50]. A multiwavelength source is required to probe all elements simultaneously [20]. A photoacoustic imaging system using the FP etalon was built and tested to demonstrate the feasibility of parallel detection by scanning a fiber tip to emulate a photodetector array [51]. This scheme to realize detector arrays can also be applied to noncontact low-coherence interferometers. The detector arrays capable of parallel detection might be technically simpler by the FP etalon than by the microring resonator which could require more optical and electronic instruments.

4. Photoacoustic endoscopy

PAE is a promising solution for the clinical need to image internal organs such as the cardiovascular system and gastrointestinal tract which are not reachable using bulky PAM setup [52]. Complementary to existing endoscopic imaging technologies such as ultrasound endoscopy, PAE produces useful anatomic and functional information which is of great value for endoscopic diagnosis. Since the

Table 1
Comparison of ultrasound detection technologies in PAM.

Detection technology	NEP (Pa)*	Band-width (MHz)	Detection Size (μm)	Photoacoustic Axial Resolution (μm)	Reference
Optical ultrasound detection					
Microring	105	350	60	<3	[12]
FP etalon	100	20	10	60 – 70**	[29]
Noncontact interferometer	NA	67	10 – 20**	20	[44,46]
Piezoelectric detector					
PVDF needle hydrophone	6000	100	75	NA	Precision Acoustics
Commercial transducer, Olympus	15	100	3000	7.6	[37]

* The NEP was measured over its corresponding bandwidth.
** Estimated values

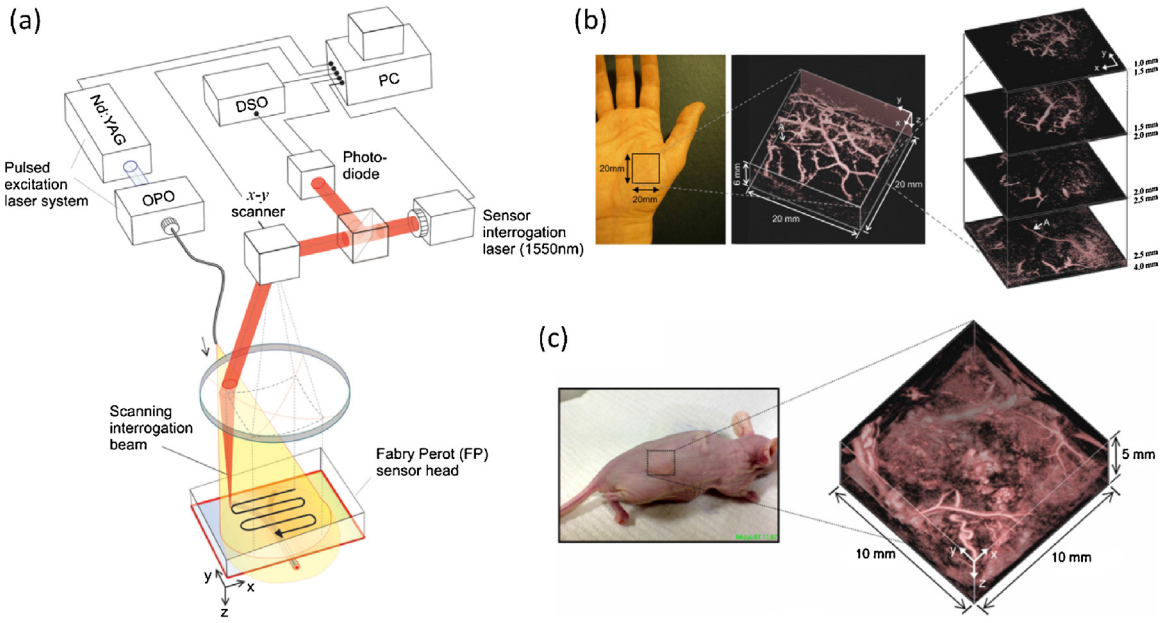

Fig. 3. AR-PAM relying on optical ultrasound detection. (a) A photoacoustic imaging system based on the raster scan over a FP sensor head, where the FP sensor head acoustically contacts and the surface of the skin [48]. Sample is placed under the FP sensor head. (b) *In vivo* photoacoustic image of the vasculature in human palm skin using an excitation wavelength of 670 nm [48]. (c) Photoacoustic image of a LS174T tumor obtained using an excitation wavelength of 650 nm [48]. Reprinted with permission from Ref. [48].

sensitivity of an optical ultrasound detector is independent of its element size, PAE based on AOPAM has a better chance to be miniaturized. There has been some progress: (1) A 5-mm probe was made using the microring resonator on a transparent substrate [13]. It had high radial resolution of ~20 μm but suffered from poor transverse resolution of 750 μm due to the lack of optical or acoustic focusing. (2) To improve transverse resolution and imaging speed of PAE, a miniature microring-based AOPAM system consisting of a microelectromechanical systems (MEMS) mirror for raster scan and a small objective lens for optical focusing was exploited for prototype study [53]. The capability of this system for high-resolution PAE was demonstrated by imaging the microvasculature of a canine bladder (Fig. 4a). (3) Dong *et al.* demonstrated an AOPAM endoscopic probe with an outer diameter of 4.5 mm (probe size) by employing a cover-slip-type microring ultrasound detector [15], as shown in Fig. 4b.

Another approach to construct a PAE probe in AOPAM form is using the FP etalon [14,54–56]. A miniature photoacoustic FP scanner was proposed [54]. The FP etalon was attached on the front side of a GRIN lens and the interrogation beam was scanned on the

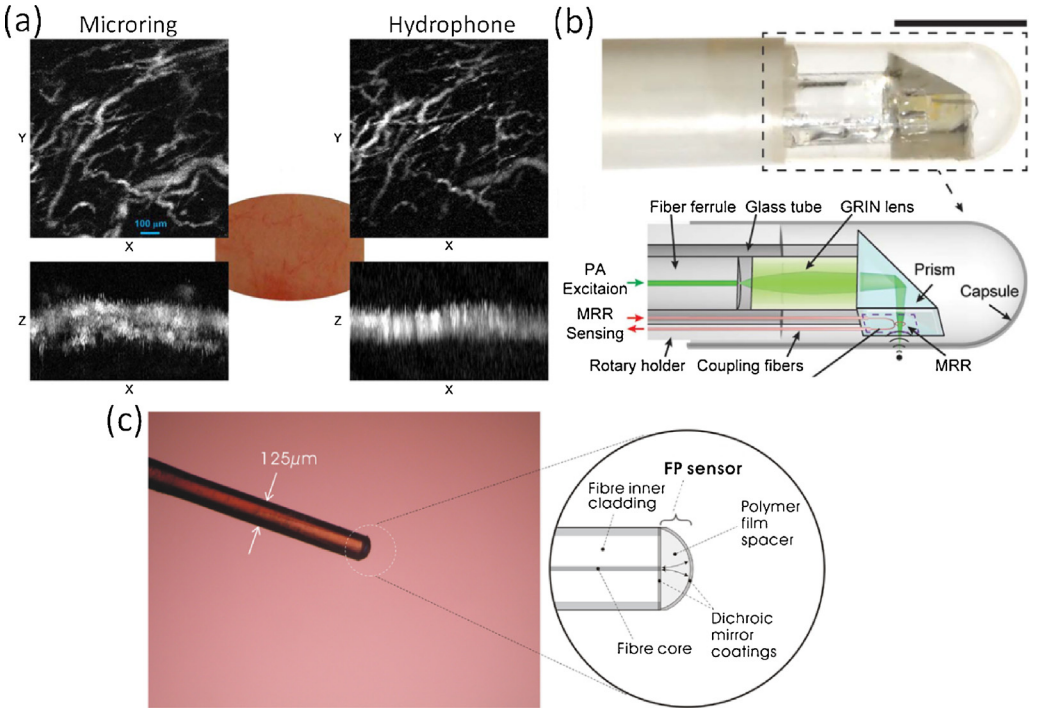

Fig. 4. PAE relying on optical ultrasound detection. (a) Photoacoustic images of the microvasculature in a mouse bladder wall obtained by a microring detector and a hydrophone [53]. (b) Photograph and schematic of a microring-based PAE probe. The outer diameter is 4.5 mm (probe size). Bar: 5 mm [15]. (c) A plano-convex FP interferometer cavity formed at the distal end of a plane cleaved fiber [14]. Reprinted with permission from Refs. [14,15,53].

back side of the GRIN lens to realize 2D mapping of photoacoustic signals. Alternatively, a fiber-optic FP ultrasound sensor for PAE was investigated [14,55,56]. Through optimized design using a plano-convex FP interferometer cavity formed at the distal end of a single-mode optical fiber (250 μm outer diameter, Fig. 4c), a high ultrasound detection sensitivity was achieved (NEP measured as tens of Pa over a 20 MHz bandwidth [56]). Potential of imaging at higher speeds by employing a bundle of these optical ultrasound detectors was proposed [55]. Besides the FP etalon, a new paradigm using coherence-restored pulse interferometry implemented with a fiber-based resonator was demonstrated and a miniaturized all-optical photoacoustic imaging catheter was showcased [57].

There are several advantages of this AOPAM-based photoacoustic probes, such as electromagnetic interference free operation and the elimination of direct connection to an amplifier circuit/system which is essential for miniaturization [53]. A higher level of miniaturization was achieved by the FP etalon (device size: 250 μm) [14] than by the microring resonator (device size: < 1 mm) [15]. This may be because the FP etalon can be fabricated on to the tip of a single fiber while two fibers with a certain separation were employed for easy probing the input and output of the microring resonator. As mentioned in Section 2, however, a much broader bandwidth was achieved by the microring resonator, offering better radial resolution (4.5 μm) for PAE imaging [15].

5. Multi-modality imaging

By integrating AOPAM with other imaging modalities, multi-parametric imaging originated from multiple contrasts, such as fluorescence and light scattering, shows great promise in providing complementary information. Owing to the superior spatial resolutions along both axial and lateral directions by AOPAM, it is suitable to integrate AOPAM with existing optical microscopy modalities which have comparable high spatial resolutions for multimodal microscopic imaging [58,59]. There have been several multimodal imaging systems built by microring-based AOPAM: (1) A fiber-optic system for viewing cells by fluorescence contrast and ambient microvasculature through optical absorption contrast was developed using a microring resonator [58], as shown in Fig. 5a. In this system, miniature components were used to demonstrate a prototype for future development of a dual-modality endoscopic probe. PAM image of the microvasculature in a rat bladder (Fig. 5b) and confocal fluorescence microscopic image of a canine bladder (Fig. 5c) were demonstrated. (2) Another system was built using a commercial inverted microscope platform [59], as shown in Fig. 5d. By integrating AOPAM with established microscopic modalities, single cell imaging with extrinsic fluorescence staining, intrinsic autofluorescence, and optical absorption was achieved simultaneously (Fig. 5e). (3) An all-optical scanhead for PAM and ultrasound multimodality imaging was demonstrated using optoacoustic generation of ultrasound and a microring resonator for acoustic detection, which can simplify integration of the two systems and miniaturize the imaging scanhead [47].

Besides the microring resonator, a combined photoacoustic tomography, OR-PAM, and OCT instrument based on the use of a FP etalon ultrasound sensor was developed for imaging biological tissues [60,61]. One advantage of using the FP etalon scanner is co-registered scan of photoacoustic detection and other imaging

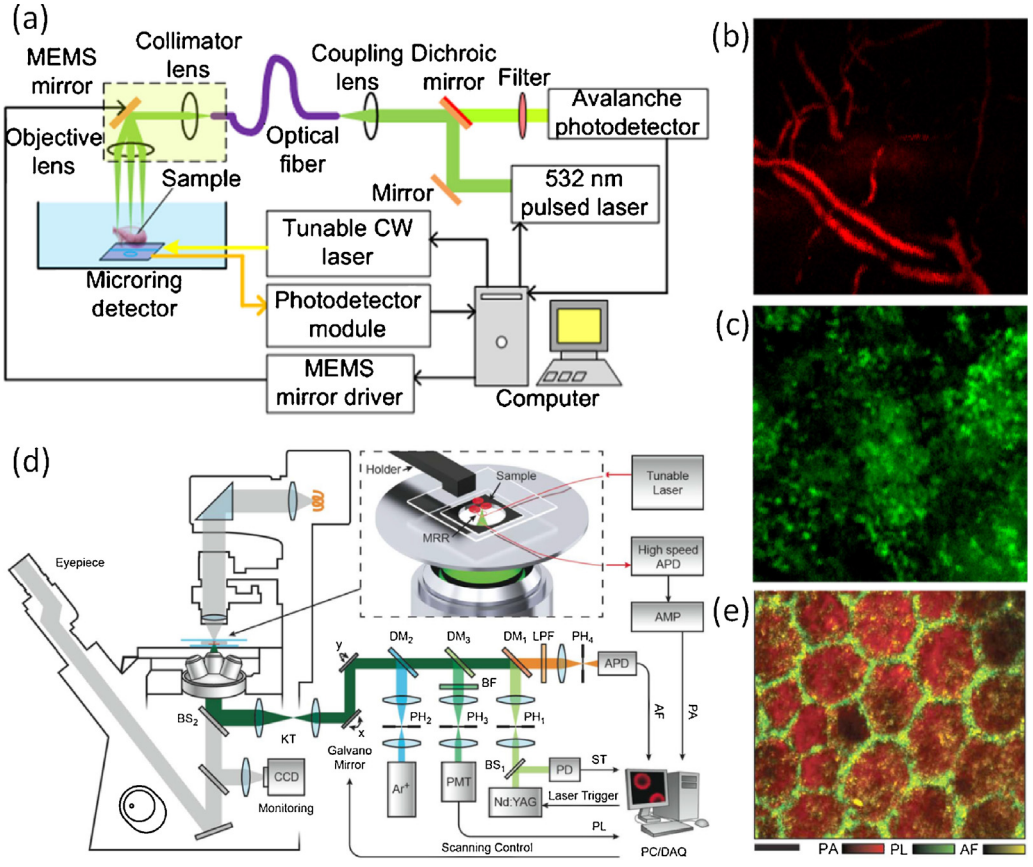

Fig. 5. Multi-modality imaging involving optical ultrasound detection. (a) Schematic diagram of a fiber-optic based PAM and confocal fluorescence microscopy dual-modality imaging system [58]. (b) PAM image of the microvasculature in a rat bladder (Imaged area: 0.9 mm × 0.9 mm) and (c) Confocal fluorescence microscopic image of a canine bladder (Imaged area: 0.6 mm × 0.6 mm) acquired by the system in (a) [58]. (d) An integrated microscopic system combining laser-scanning confocal microscopy and PAM. The inset illustrates a magnified view of the placement of the fiber coupled microring ultrasonic detector and specimen [59]. (e) Overlaid image of three modalities (PA: photoacoustic, PL: Phalloidin fluorescence, AF: autofluorescence) acquired simultaneously by the system in (d). Scale bar: 10 μm [59]. Reprinted with permission from Refs. [58,59].

modalities, e.g., OCT, which has the potential for simultaneous multi-modality scan [60,61]. A noncontact integrated PAM and OCT dual-mode imaging system was presented using a Michelson detector [46]. In addition, Berer *et al.* demonstrated a dual mode photoacoustic and ultrasonic microscopy with its acoustic resolution provided by an optical ring-shaped detector based on a Mach-Zehnder interferometer [62].

6. Summary

In summary, we have reviewed the characteristics and applications of AOPAM imaging systems based on different optical ultrasound detection technologies. AOPAM offers the following unique features: (1) AOPAM enables high detection sensitivity with a small element size, leading to significant improvement in maximum imaging depth, field of view for laser-scanning OR-PAM, spatial resolutions for digitally-focusing AR-PAM, and miniaturization for PAE implementations. (2) AOPAM provides a bandwidth of hundreds of MHz, which improves axial resolving ability to achieve isometric spatial resolutions along both axial and lateral directions. (3) AOPAM detection sensitivity is independent of its sensing element size. (4) AOPAM array configuration is capable of fast or even parallel detection for real-time imaging.

For OR-PAM applications, imaging systems employing different optical detection such as microring resonators, FP etalon, and noncontact interferometers have been demonstrated. So far, the ultrabroad bandwidth (350 MHz) with high sensitivity has been achieved only by the microring resonator [12], suggesting its strength in offering high axial resolution over other optical ultrasound detection technologies. However, the element size reduction (e.g., from 60 μm to ~10 μm) of the microring is impeded because its detection sensitivity cannot be maintained due to high bending loss, limiting the field of view in laser-scanning OR-PAM. Similarly, in AR-PAM applications, the microring resonator supplies much wider bandwidth for multiscale imaging. Typically, a single element microring detector is mechanically scanned, hindering the microring from fast data acquisition. By contrast, fast detection can be realized using the FP etalon and the noncontact interferometer by scanning the interrogation beam [26]. Another application is to miniaturize the AOPAM system to image internal organs. A fiber-optic FP etalon sensor with a device size of 250 μm has been achieved [14], and a slightly larger device size (< 1 mm) of the microring detector was demonstrated due to two fibers used for probing the microring [15]. By integrating the microring detector with the components used for excitation light delivery and focusing, the PAE probe with a 4.5-mm diameter (probe size) has been demonstrated [15]. By contrast, since the excitation light delivery can be realized by using a dual-clad fiber [14], it is more promising to use the FP etalon to make an even smaller PAE probe, possibly < 1 mm (probe size), for intravascular photoacoustic imaging. However, there is a trade-off between bandwidth and sensitivity. AOPAM integrated with other imaging modalities can provide complementary contrasts. The microring resonator provides isometric spatial resolutions that is also comparable to that of existing optical microscopic modalities such as fluorescence confocal imaging, making microring-based multi-modality imaging system more promising.

The improvement of the optical ultrasound detection technologies in system implementation will eventually lead AOPAM to commercialization. For the microring resonator, further reduction of element size without compromising the detection sensitivity is advantageous to enhance the field of view in laser-scanning OR-PAM. Besides, small element size is necessary to make denser microring arrays for fast data acquisition [30]. Further miniaturization of the microring device size to less than 1 mm may be achieved by using a dual-clad fiber to probe the input and output of the microring. For the FP etalon, wider bandwidth without sacrificing sensitivity helps to open up broad applications such as intravascular photoacoustic imaging. The noncontact interferometer has the potential for PAE implementation. Systems capable of parallel, real-time data acquisition are desired for further improving the imaging speed.

The recent progress in AOPAM has led to a rapid growth of biomedical photoacoustic technology during the past decade. The aforementioned characteristics of optical ultrasound detection, such as a miniature size and high detection sensitivity over a broad bandwidth, feature largely in AOPAM and its potential applications in biomedicine. With advances in optical ultrasound detection technologies, we believe that the novel AOPAM systems will continue to be upgraded and have great potential for improvements in sensitivity, spatial resolutions, and penetration depth in the coming years.

Conflict of interest

None.

Acknowledgement

Support from NIH Grants No. R01 AR060350 and R01 CA186769 are gratefully acknowledged.

References

[1] L.V. Wang, Multiscale photoacoustic microscopy and computed tomography, Nature Photon 3 (9) (2009) 503–509.
[2] L.V. Wang, S. Hu, Photoacoustic tomography: in vivo imaging from organelles to organs, Science 335 (6075) (2012) 1458–1462.
[3] X. Wang, Y. Pang, G. Ku, X. Xie, G. Stoica, L.V. Wang, Noninvasive laser-induced photoacoustic tomography for structural and functional in vivo imaging of the brain, Nat Biotechnol 21 (2003) 803–806.
[4] M. Xu, Y. Xu, L.V. Wang, Time-domain reconstruction algorithms and numerical simulations for thermoacoustic tomography in various geometries, IEEE Trans Biomed Eng 50 (9) (2003) 1086–1099.
[5] H.F. Zhang, K. Maslov, G. Stoica, L.V. Wang, Functional photoacoustic microscopy for high-resolution and noninvasive in vivo imaging, Nat Biotechnol 24 (7) (2006) 848–851.
[6] K. Maslov, H.F. Zhang, S. Hu, L.V. Wang, Optical-resolution photoacoustic microscopy for in vivo imaging of single capillaries, Opt Lett 33 (9) (2008) 929–931.
[7] Y. Xu, L.V. Wang, Time reversal and its application to tomography with diffracting sources, Phys Rev Lett 92 (3) (2004) 033902.
[8] M.H. Xu, L.V. Wang, Universal back-projection algorithm for photoacoustic computed tomography, Phys Rev E 71 (1) (2005) 016706.
[9] P. Kuchment, L. Kunyansky, Mathematics of photoacoustic and thermoacoustic tomography, in: O. Imaging, Scherzer (Eds.), Handbook of mathematical methods., Springer, New York, NY u.a, 2011, pp. 817–866.
[10] K.A. Snook, J.Z. Zhao, C.H. Alves, J.M. Cannata, W.H. Chen, R.J. Meyer Jr., T.A. Ritter, K.K. Shung, Design, fabrication, and evaluation of high frequency, single-element transducers incorporating different materials, IEEE Trans Ultrason Ferroelectr Freq Control 49 (2) (2002) 169–176.
[11] T. Ling, S.L. Chen, L.J. Guo, High-sensitivity and wide-directivity ultrasound detection using high Q polymer microring resonators, Appl Phys Lett 98 (20) (2011) 204103.
[12] C. Zhang, T. Ling, S.L. Chen, L.J. Guo, Ultrabroad bandwidth and highly sensitive optical ultrasonic detector for photoacoustic imaging, ACS Photonics 1 (11) (2014) 1093–1098.
[13] S.L. Chen, T. Ling, H.W. Baac, L.J. Guo, Photoacoustic endoscopy using polymer microring resonators, Proc SPIE 7899 (2011), 78992T..
[14] E.Z. Zhang, P.C. Beard, A miniature all-optical photoacoustic imaging probe, Proc SPIE 7899 (2011), 78991F..
[15] B. Dong, S. Chen, Z. Zhang, C. Sun, H.F. Zhang, Photoacoustic probe using a microring resonator ultrasonic sensor for endoscopic applications, Opt Lett 39 (15) (2014) 4372–4375.
[16] Y. Wang, C. Li, R.K. Wang, Noncontact photoacoustic imaging achieved by using a low-coherence interferometer as the acoustic detector, Opt. Lett 36 (20) (2011) 3975–3977.
[17] G. Rousseau, A. Blouin, J.P. Monchalin, Non-contact photoacoustic tomography and ultrasonography for tissue imaging, Biomed Opt Express 3 (1) (2012) 16–25.
[18] A. Hochreiner, J. Bauer-Marschallinger, P. Burgholzer, B. Jakoby, T. Berer, Non-contact photoacoustic imaging using a fiber based interferometer with optical amplification, Biomed Opt Express 4 (11) (2013) 2322–2331.

[19] J.P. Monchalin, Optical detection of ultrasound, IEEE Trans Ultrason Ferroelectr Freq Control 33 (5) (1986) 485–499.
[20] C.Y. Chao, S. Ashkenazi, S.W. Huang, M. O'Donnell, L.J. Guo, High-frequency ultrasound sensors using polymer microring resonators, IEEE Trans Ultrason Ferroelectr Freq Control 54 (5) (2007) 957–965.
[21] S.L. Chen, T. Ling, S.W. Huang, H.W. Baac, L.J. Guo, Photoacoustic correlation spectroscopy and its applications to low speed flow measurement, Opt Lett 35 (8) (2010) 1200–1202.
[22] S.L. Chen, Y.C. Chang, C. Zhang, J.G. Ok, T. Ling, M.T. Mihnev, T.B. Norris, L.J. Guo, Efficient real-time detection of terahertz pulse radiation based on photoacoustic conversion by carbon nanotube nanocomposite, Nature Photon 8 (2014) 537–542.
[23] P.C. Beard, F. Perennes, T.N. Mills, Transduction mechanisms of the Fabry–Perot polymer film sensing concept for wideband ultrasound detection, IEEE Trans Ultrason Ferroelectr Freq Control 46 (6) (1999) 1575–1582.
[24] S. Ashkenazi, Y. Hou, T. Buma, M. O'Donnell, Optoacoustic imaging using thin polymer etalon, Appl Phys Lett 86 (13) (2005) 134102.
[25] Y. Hou, J.S. Kim, S. Ashkenazi, S.W. Huang, L.J. Guo, M. O'Donnell, Broadband all-optical ultrasound transducers, Appl Phys Lett 91 (2007) 073507.
[26] E. Zhang, J. Laufer, P. Beard, Backward-mode multiwavelength photoacoustic scanner using a planar Fabry–Perot polymer film ultrasound sensor for high-resolution three-dimensional imaging of biological tissues, Appl Opt 47 (4) (2008) 561–577.
[27] P. Morris, A. Hurrell, A. Shaw, E. Zhang, P. Beard, A Fabry-Perot fiber-optic ultrasonic hydrophone for the simultaneous measurement of temperature and acoustic pressure, J Acoust Soc Am 125 (6) (2009) 3611–3665.
[28] Y. Hou, S.W. Huang, S. Ashkenazi, R. Witte, M. O'Donnell, Thin polymer etalon arrays for high-resolution photoacoustic imaging, J Biomed Opt 13 (6) (2008) 064033.
[29] T.J. Allen, E. Zhang, P.C. Beard, Large-field-of-view laser-scanning OR-PAM using a fibre optic sensor, Proc SPIE 9323 (2015), 93230Z.
[30] C. Zhang, S.L. Chen, T. Ling, L.J. Guo, Review of imprinted polymer microring as ultrasound detector: design, fabrication, and characterization, IEEE Sensors J 15 (2015) 3241–3248.
[31] C. Zhang, K. Maslov, L.V. Wang, Subwavelength-resolution label-free photoacoustic microscopy of optical absorption in vivo, Opt Lett 35 (19) (2010) 3195–3197.
[32] J. Yao, L. Wang, C. Li, C. Zhang, L.V. Wang, Photoimprint photoacoustic microscopy for three-dimensional label-free subdiffraction imaging, Phys Rev Lett 112 (2014) 014302.
[33] A. Danielli, K. Maslov, A. Garcia-Uribe, A.M. Winkler, C. Li, L. Wang, Y. Chen, G.W. Dorn II, L.V. Wang, Label-free photoacoustic nanoscopy, J Biomed Opt 19 (8) (2014) 086006.
[34] T. Ling, S.L. Chen, L.J. Guo, Fabrication and characterization of High Q polymer micro-ring resonator and its application as a sensitive ultrasonic detector, Opt Express 19 (2) (2011) 861–869.
[35] Z. Xie, S.L. Chen, T. Ling, L.J. Guo, P.L. Carson, X. Wang, Pure optical photoacoustic microscopy, Opt Express 19 (10) (2011) 9027–9034.
[36] Z. Xie, S. Jiao, H.F. Zhang, C.A. Puliafito, Laser-scanning optical-resolution photoacoustic microscopy, Opt Lett 34 (12) (2009) 1771–1773.
[37] C. Zhang, K. Maslov, J. Yao, L.V. Wang, In vivo photoacoustic microscopy with 7.6-m axial resolution using a commercial 125 MHz ultrasonic transducer, J Biomed Opt 17 (11) (2012) 116016.
[38] H. Li, B. Dong, Z. Zhang, H.F. Zhang, C. Sun, A transparent broadband ultrasonic detector based on an optical micro-ring resonator for photoacoustic microscopy, Sci Rep 4 (2014) 4496.
[39] Z. Zhang, B. Dong, H. Li, F. Zhou, H.F. Zhang, C. Sun, Theoretical and experimental studies of distance dependent response of micro-ring resonator-based ultrasonic detectors for photoacoustic microscopy, J Appl Phys 116 (14) (2014) 144501.
[40] S.L. Chen, T. Ling, L.J. Guo, Low-noise small size microring ultrasonic detectors for high resolution photoacoustic imaging, J Biomed Opt 16 (2011) 056001.
[41] P. Hajireza, K. Krause, M. Brett, R. Zemp, Glancing angle deposited nanostructured film Fabry-Perot etalons for optical detection of ultrasound, Opt Express 21 (5) (2013) 6391–6400.
[42] P. Hajireza, J. Sorge, M. Brett, R. Zemp, In vivo optical resolution photoacoustic microscopy using glancing angle-deposited nanostructured Fabry-Perot etalons, Opt Lett 40 (7) (2015) 1350–1353.
[43] J.N. Caron, P. Kunapareddy, Atypical Applications for Gas-coupled Laser Acoustic Detection, J Phys Conf Ser 520 (2014) 012022.
[44] Z. Chen, S. Yang, Y. Wang, D. Xing, Noncontact broadband all-optical photoacoustic microscopy based on a low-coherence interferometer, Appl Phys Lett 106 (2015) 043701.
[45] A. Sampathkumar, P.V. Chitnis, R.H. Silverman, An all-optical photoacoustic microscopy system for remote, noncontact characterization of biological tissues, Proc Meet Acoust 19 (2013) 075009.
[46] Z. Chen, S. Yang, Y. Wang, D. Xing, All-optically integrated photo-acoustic microscopy and optical coherence tomography based on a single Michelson detector, Opt Lett 40 (12) (2015) 2838–2841.
[47] B.Y. Hsieh, S.L. Chen, T. Ling, L.J. Guo, P.C. Li, All-optical scanhead for ultrasound and photoacoustic imaging—Imaging mode switching by dichroic filtering, Photoacoustics 2 (1) (2014) 39–46.
[48] E.Z. Zhang, J.G. Laufer, R.B. Pedley, P.C. Beard, In vivo high-resolution 3D photoacoustic imaging of superficial vascular anatomy, Phys Med Biol. 54 (4) (2009) 1035–1046.
[49] J. Liu, Z. Tang, Y. Wu, Y. Wang, Rapid and noncontact photoacoustic tomography imaging system using an interferometer with high-speed phase modulation technique, Rev Sci Instrum 86 (2015) 044904.
[50] A. Maxwell, S.W. Huang, T. Ling, J.S. Kim, S. Ashkenazi, L.J. Guo, Polymer microring resonators for high-frequency ultrasound detection and imaging, IEEE J Sel Top Quantum Electron 14 (1) (2008) 191–197.
[51] S.W. Huang, Y. Hou, S. Ashkenazi, M. O'Donnell, High-resolution ultrasonic imaging using an etalon detector array, Appl Phys Lett 93 (2008) 113501.
[52] L.V. Wang, Prospects of photoacoustic tomography, Med Phys 35 (12) (2008) 5758–5767.
[53] S.L. Chen, Z. Xie, T. Ling, L.J. Guo, X. Wei, X. Wang, Miniaturized all-optical photoacoustic microscopy based on microelectromechanical systems mirror scanning, Opt Lett 37 (20) (2012) 4263–4265.
[54] C. Sheaff, N. Lau, H. Patel, S.W. Huang, S. Ashkenazi, Photoacoustic imaging endoscope, Proc IEEE Eng Med Biol Soc 2009 (2009) 1983–1986.
[55] C. Sheaff, S. Ashkenazi, A fiber optic optoacoustic ultrasound sensor for photoacoustic endoscopy, IEEE International Ultrasonics Symposium (2010) 2135–2138.
[56] E.Z. Zhang, P.C. Beard, Characteristics of optimized fibre-optic ultrasound receivers for minimally invasive photoacoustic detection, Proc SPIE 9323 (2015) 932311.
[57] A. Rosenthal, S. Kellnberger, D. Bozhko, A. Chekkoury, M. Omar, D. Razansky, V. Ntziachristos, Sensitive interferometric detection of ultrasound for minimally invasive clinical imaging applications, Laser Photon Rev 8 (3) (2014) 450–457.
[58] S.L. Chen, Z. Xie, L.J. Guo, X. Wang, A fiber-optic system for dual-modality photoacoustic microscopy and confocal fluorescence microscopy using miniature components, Photoacoustics 1 (2) (2013) 30–35.
[59] B. Dong, H. Li, Z. Zhang, K. Zhang, S. Chen, C. Sun, H.F. Zhang, Isometric multimodal photoacoustic microscopy based on optically transparent micro-ring ultrasonic detection, Optica 2 (2) (2015) 169–176.
[60] E.Z. Zhang, J. Laufer, B. Považay, A. Alex, B. Hofer, W. Drexler, P. Beard, Multimodal simultaneous photoacoustic tomography, optical resolution microscopy and OCT system, Proc SPIE 7564 (2010), 75640U..
[61] M. Liu, N. Schmitner, M.G. Sandrian, B. Zabihian, B. Hermann, W. Salvenmoser, D. Meyer, W. Drexler, In vivo three dimensional dual wavelength photoacoustic tomography imaging of the far red fluorescent protein E2-Crimson expressed in adult zebrafish, Biomed Opt Express 4 (10) (2013) 1846–1855.
[62] T. Berer, H. Grun, J. Bauer-Marschallinger, P. Burgholzer, K. Passler, R. Nuster, G. Paltauf, Dual mode photoacoustic/acoustic microscopy with optical generation and detection, IEEE International Ultrasonics Symposium (2012) 1–4.

Sung-Liang Chen is currently an Assistant Professor at the University of Michigan-Shanghai Jiao Tong University Joint Institute, Shanghai, China. He received his Ph.D. degree in electrical engineering at the University of Michigan, Ann Arbor, and postdoctoral training at the University of Michigan Medical School. His research interests include optical resonators for sensing applications, optical imaging systems, and biomedical photoacoustic imaging. He is the recipient of the Thousand Talents Plan given by the Chinese Recruitment Program of Global Experts for young professionals and Shanghai Pujiang Talent Award.

L. Jay Guo started his academic career at the University of Michigan in 1999, and is currently a professor of Electrical Engineering and Computer Science, with joint appointment in Applied Physics, Mechanical Engineering, Macomolecular Science and Engineering. He has 190 refereed journal publications with over 13,500 citations. Many published work from his lab have been reported by numerous media. His group's researches include polymer-based photonic devices and sensor applications, laser generated ultrasound, organic and hybrid photovoltaics, plasmonic nanophotonics, and roll to roll nanomanufacturing technologies.

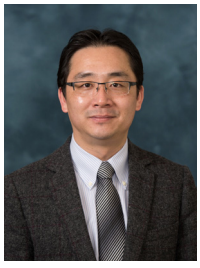

Dr. Xueding Wang is currently an Associate Professor at the Department of Biomedical Engineering, University of Michigan, holding an Adjunct Associate Professor position at the Department of Radiology. Before working as an independent principle investigator, Dr. Wang received his Ph.D. at Texas A&M University under the supervision of Dr. Lihong Wang, and Postdoctoral training at the University of Michigan. Dr. Wang has extensive experience in imaging system development and adaptation of novel diagnostic technology to laboratory research and clinical managements, especially those involving light and ultrasound. Sponsored by NIH, NSF, DoD and other funding agencies, his research has led to over 100 + peer-reviewed publications. At the University of Michigan Medical School, a major part of his research is focused on clinical applications of photoacoustic imaging. Dr. Wang is the recipient of the Sontag Foundation Fellow of the Arthritis National Research Foundation in 2005, Joint Research Fund for Overseas Chinese Scholars and Scholars in Hong Kong and Macao from National Science Foundation of China in 2011, and the Distinguished Investigator Award of the Academy of Radiology Research in 2013. He is also sitting on the editorial boards of scientific journals including Photoacoustics, Ultrasonic Imaging, and Journal of Lightwave Technology.